Nanotechnology Perceptions
ISSN 1660-6795
www.nano-ntp.com

Development of Solar Dryer Combined with Infrared Radiation for Phlai (Zingiber Montanum (J. Koenig) Link ex A. Dietr.) Drying

Thanin Rudchapo, Pattanapol Meena

Department of Physics, Faculty of Science, Mahasarakham University, 44150 Mahasarakham, Thailand
Email: thanin0003@gmail.com

The aims of this work were to develop a solar dryer combined with infrared radiation for Phlai drying and to investigate the performance of the developed dryer. The dryer consisted of a drying chamber, a source of uneven infrared radiation, a 70% thermal energy recovery unit, a solar thermal energy collector, and a latent thermal energy storage unit. Experiments followed a factorial design, with Phlai interior temperatures (PIT) of 50, 60, and 70 °C and infrared power (IRP) levels of 500, 1000, and 1500 Watts (W). The results showed that the drying rate (DR), specific electrical energy consumption (SEEC), and the solar collector efficiency (ηcoll) ranged from 0.0047 to 0.0123 kgwaterh-1, 1.58 to 14.15 kW, and 53.36 to 83.69%, respectively. The optimum IRP was 1500 W. The optimum PIT could be separated into two cases: for saving energy reduction, it was 50 °C, whereas for short drying time, it was 70 °C.

Keywords: Drying performance, Energy reduction, Infrared drying, Paraffin wax, Solar drying

1. Introduction

Thailand is an agriculture country in Southeast Asia with relatively high solar irradiance levels (the average daily solar irradiation is 18 $MJ(m^2\text{-day})^{-1}$). Therefore, solar energy technology is well-suited for use in agricultural processes, particularly post-harvest management. Currently, solar thermal drying technology is one of the post-harvest management methods that is very popular because it is clean, energy-efficient, and non-polluting [1]. Also, the temperature of the drying air in the solar dryer ranges from 45 to 60 °C [2], which is perfect for drying a variety of agro-food products. However, applying solar thermal drying technology to agricultural products often presents several issues, such as uneven solar irradiation and limited working hours compared to other energy sources [3]. This system requires a long drying time, and its performance decreases during off-sunshine hours [4], which impacts product quality

[5, 6]. Therefore, the development of a hybrid solar dryer was necessary to solve these problems. Currently, infrared radiation drying is a method that has received a lot of attention and is widely accepted for enhancing energy performance, retaining quality of product, and shortening the drying period [7, 8]. Another method to reduce the energy consumption was to apply an uneven form of on-off infrared source [9]. Furthermore, installing a thermal energy storage unit [10] and a thermal energy recovery unit [11] can also improve the efficiency of solar dryers and solve the issue of uneven solar irradiation. There have been studies attempting to enhance the performance of solar dryers. Ziaforoughi and Esfahani [5] studied a solar collector-assisted intermittent infrared dryer. They found electrical energy consumption decreased by 40%–69%. Additionally, drying time decreased by 31–52% compared to that with an intermittent infrared dryer. Rabha and Muthukumar, [2] examined convection solar dryers in combination with shell and tube thermal energy storage units, with paraffin wax as the thermal energy storage material. They found that drying times were reduced, and it lessened the temperature fluctuations of the drying air during cloud cover or when there was no sunlight. Aktas et al. [11] studied the drying of melons with a solar dryer combined with infrared radiation and thermal energy recovery with the use of a heat exchanger. They found that it could increase energy in the dryer by up to 23–28% of the total input energy. While studies have aimed to enhance the performance of solar dryers using various techniques, no research has yet improved solar dryer performance by integrating thermal energy storage, thermal energy recovery, and uneven infrared drying in the same solar dryer system. These discoveries could serve as guidelines for developing a hybrid solar dryer.

Zingiber montanum (J. Koenig) Link ex A. Dietr., also known as "Phlai" by Thais [12], is an aromatic herb plant in the Zingiberaceae family [13]. Phlai's rhizome includes essential oils, phenylbutanoids, and cassumunoids, which have been reported to have anti-inflammatory properties [14]. Thai medicine utilizes Phlai to treat sprains, inflammation, muscle aches, rheumatism, etc. [15]. After harvest, the Phlai's moisture content can be as much as 400% d.b. [16]. When stored for a long time, important substances in essential oils deteriorate. Therefore, water removal is necessary to prevent spoilage and to slow down the enzymatic reactions that occur within the Phlai. There have been few studies of water removal from Phlai. Mahayothee et al. [17] investigated the influence of drying technique and drying temperature on drying rate and bioactive components in Phlai slices dried with a hot air dryer at 40, 50, 60, 70, and 80 °C, a greenhouse solar dryer, and by sun drying. They found that increasing the drying temperature of the hot air-drying process accelerated the drying rate. However, the high drying temperature decreased the yield of essential oils. Furthermore, it was discovered that the dried samples from the greenhouse solar dryer and the hot air dryer had marginally greater antioxidant capabilities than the samples from sun drying. Meunathasa et al. [16] studied the effect of drying temperatures on the quality of Phlai rhizome. Phlai were dried in a hot air oven at a drying temperature of 40, 50, 60, 80, and 100 °C. They found that high-temperature drying removed moisture more quickly than low-temperature drying. The decrease in volatile oil content was significantly related to increased drying temperature. According to a review of the limited literature on water removal from Phlai, no study has yet investigated using a hybrid solar dryer for Phlai drying process. Addressing this gap was another objective of the present study.

The literature review offers guidelines for enhancing the performance of hybrid solar dryers for Phlai drying. Therefore, the objectives of this work were to: 1) develop a hybrid solar dryer for Phlai drying that integrates thermal energy recovery (without a heat exchanger), thermal energy storage, and uneven infrared drying; and 2) investigate the performance of the developed dryer. The experiments were conducted at Phlai interior temperatures (PIT) of 50, 60, and 70 °C and infrared power (IRP) levels of 500, 1000, and 1500 watts (W).

2. Materials and methods

2.1 Description of developed dryer

The developed dryer for this work was a hybrid solar dryer type that had the following main components: a solar thermal energy collector, a drying chamber, an uneven infrared heater, a thermal energy storage unit, and a thermal energy recovery unit. The specifics of each component of the developed dryers are as follows:

The solar thermal energy collector operates on the principle of the greenhouse effect [18]. The solar collector area was determined based on the heat energy required for the drying system (including the thermal energy needed to evaporate water from the product and the thermal energy required for the thermal energy storage unit) and the solar radiation intensity (Wm^{-2}) of Thailand. In this work, the dimensions of the solar thermal energy collector were 1.00 m in width, 2.00 m in length, and 0.15 m in height. An aluminum flat plate absorber was installed inside, and the aluminum fins were fixed at the same height and at a 30° angle to the direction of airflow [19]. To increase the rate of solar radiation energy absorption, the inside surface of the solar thermal energy collector was painted matte black [20, 21], as shown in Figure 1(B). A 4 mm-thick transparent polycarbonate sheet covered the collector's top, and this prevented heat from escaping from the surface of the collector [22]. 6.5-mm-thick black nitrile rubber insulation was used to cover the collector's sides and underside. 6 fans (d.c. 12 volts) were installed on the solar thermal energy collector to provide air circulation. A photovoltaic panel (STP185S-Ad/24) was utilized to provide the necessary energy for the fan.

The drying chamber, where the evaporation process of water from the Phlai slices occurred, measured a width of 30 cm, a length of 40 cm, and a height of 30 cm. It was constructed of a 0.35 mm-thick galvanized steel sheet with black nitrile rubber insulation covering. The inside of the drying chamber was lined with aluminum foil to reflect the infrared radiation onto the Phlai slices [23]. An infrared ceramic plate heater was installed on top of the inside drying chamber. Under the infrared heater, a wire mesh drying tray measuring 10×20 cm2 was placed. The distance between the infrared heater and drying tray was set at 20 cm to provide a thorough distribution of infrared radiation, as shown in (Figure 2). The operation of the infrared heater was controlled by the PIT, which turned off when it reached the preset temperature. It would then turn on again when the PIT dropped below the preset temperature [11].

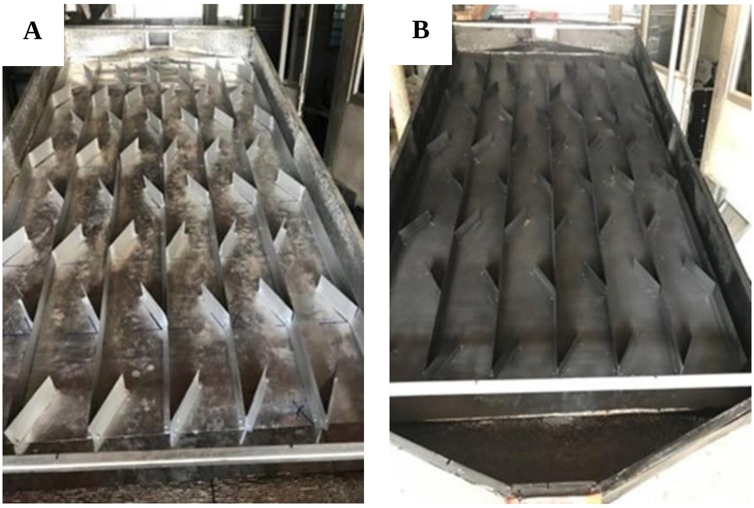

Figure 1 Inside characteristics of a solar thermal energy collector are shown in A) the before paint matte black and B) the after paint matte black.

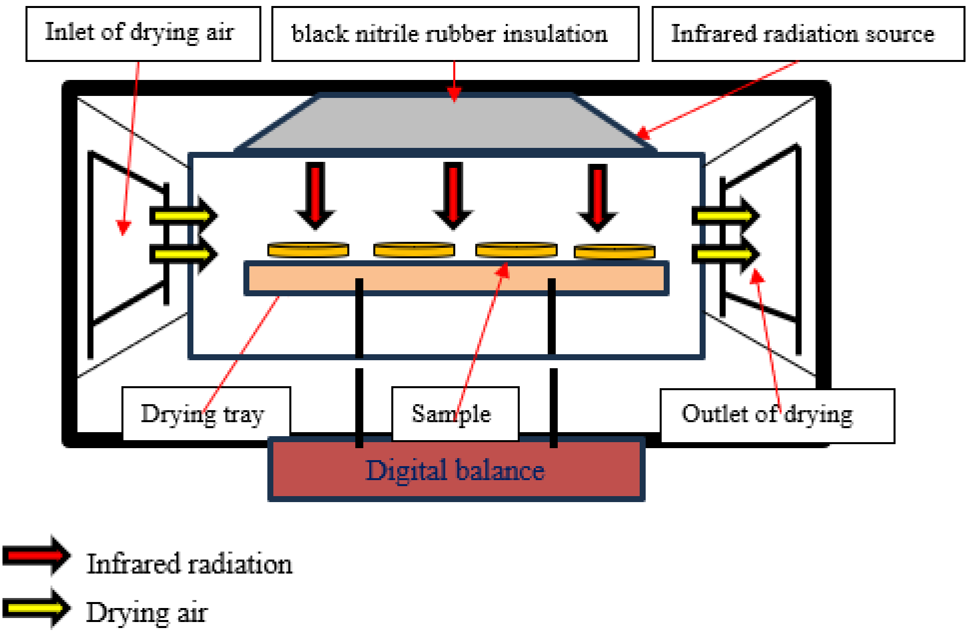

Figure 2 Features inside the drying chamber.

The drying system maintained a constant drying temperature using shell and tube latent thermal energy storage units, with paraffin wax serving as the thermal energy storage material [24]. The amount of paraffin wax used in this drying system was determined based on the heat energy required to evaporate water from the product. The shell of the thermal energy storage unit was constructed from a 2 mm-thick mild steel sheet and measured a width of 10 cm, a length of 10 cm, and a height of 13 cm. Nine copper pipes, each 13 cm in length and 2.54 cm in diameter, were fitted through the shell. The gap between the shell and the tubes was filled with 700 g of paraffin wax (the amount of paraffin wax was determined based on the thermal energy needed to evaporate water from the product). A diagram of the shell and tube thermal energy storage unit is shown in (Figure 3).

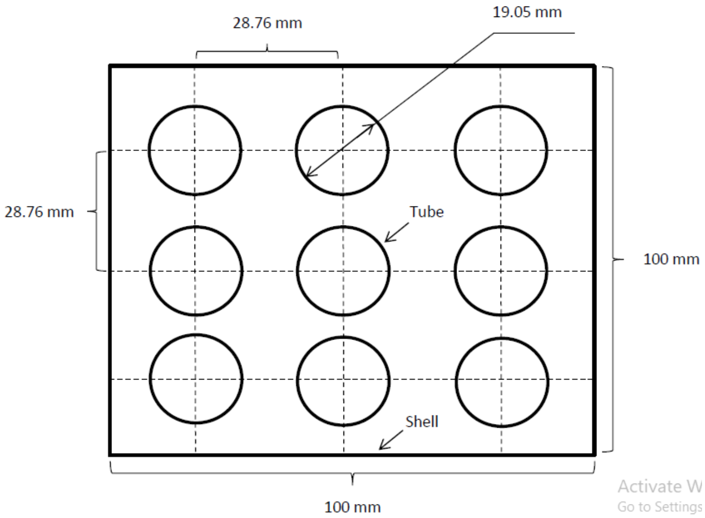

Figure 3 Diagram for the thermal energy storage unit.

Waste thermal energy recovery involves the conduction of residual thermal energy from the production process back into the production process itself. It represents a cost-effective use of energy, leading to reductions in overall energy consumption [25], energy costs, and CO_2 emissions. In this study, 70% of the waste thermal energy generated during the drying process [26] was effectively utilized by being transferred back to the solar thermal energy collector.

2.2. Sample preparation

The Phlai samples were cleaned and stored refrigerated at +4 °C [27]. Before each experiment, the samples were stored at room temperature for 1 hour [11]. Subsequently, the samples were sliced into 2 mm-thick slices using a slicing machine. The oven drying at 105 °C for 48 h was conducted to determine the moisture content in the samples. The moisture content values were calculated on a dry basis (d.b.).

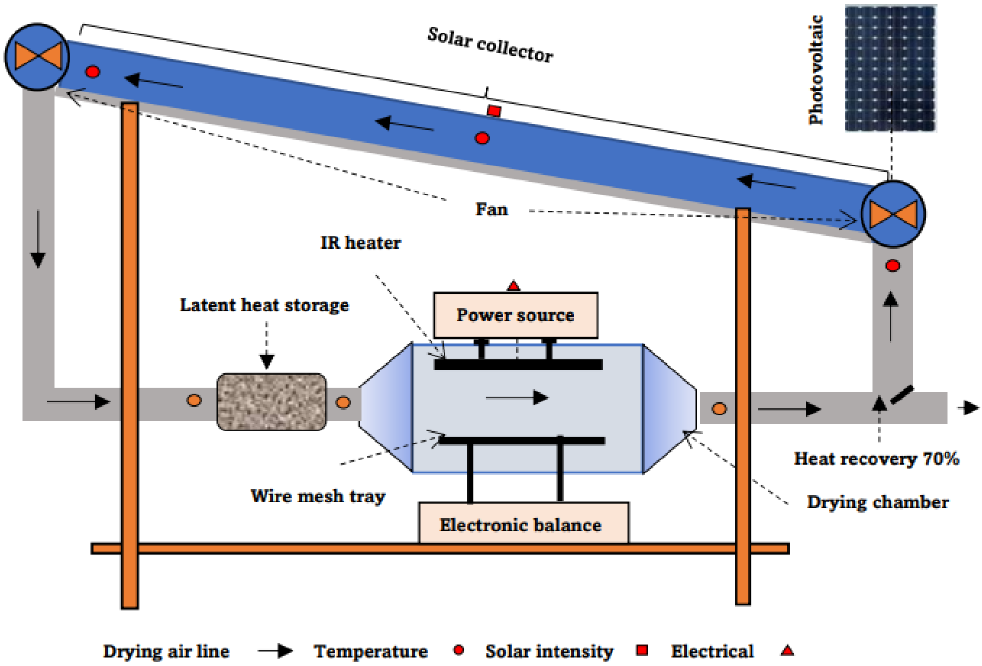

Figure 4 Measurement points of air temperature, electrical energy consumption, and solar radiation intensity.

2.3. Experiment procedure

The studies were conducted in the Mahasarakham Province of Thailand between December 2019 and May 2020. The drying experiments were carried out from 9:00 a.m. to 5:00 p.m. In each drying experiment, 100 g of phlai slices were evenly distributed in the drying tray. The experiment was conducted at Phlai interior temperatures (PIT) of 50, 60, and 70 °C, with a temperature probe (thermocouple) inserted into the Phlai slices, infrared power levels (IRP) of 500, 1000, and 1500 W, and a drying air velocity of 0.4 m/s. Changes in the sample's mass were recorded every 15 minutes using a digital balance (PA2102C/OHAUS, precision 0.01 g) until the sample's moisture content reached approximately 13% d.b. The experiments were replicated three times.

During the experiment, the drying air temperature at different points inside the dryer was recorded every 15 minutes; these included the ambient temperature (T_{amb}), temperature within the solar collector {inlet temperature (T_{ci}), center temperature (T_{cc}), outlet temperature (T_{co})}, thermal energy storage's inlet temperature (T_{tsi}), drying chamber's inlet temperature (T_{di}), drying chamber's outlet temperature (T_{do}), and phlai interior temperature. All of these temperatures were measured using type K thermocouples (WCA-G, accuracy: ±2.2 °C). A power quality meter (Fluke 1735 three-phase power quality logger) was used to measure the electrical energy consumption of the infrared radiation source. The intensity of solar radiation (I) was measured with a solar power meter (TES-1333R, accuracy typically within ±10 Wm^{-2}). The speed of the air moving through the solar collector and drying chamber was measured with a hotwire anemometer (TESTO 425, precision: 0.01 ms^{-1}).

2.4. Analyses

The Phlai's moisture content can be evaluated using the following dry basis expression:

$$M_d = \frac{w-d}{d} \times 100\% \quad (1)$$

Where M_d is the moisture contents (dry bisis), w is wet mass (kg), and d is dry mass (kg).

The parameters drying rate (DR), solar collector efficiency (η_{coll}), and specific electrical energy consumption (SEEC) were used to evaluate the developed dryer's performance. The details and methods for calculating these parameters are given below.

2.4.1 The DR shows the ratio of the quantity of water evaporated from the drying material per time unit, which was defined as follows:

$$DR = \frac{M_i - M_f}{t_d} \quad (2)$$

where M_i is the initial mass (kg), M_f is the final mass (kg), and t_d is the drying time (h).

2.4.2 The η_{coll} was determined as the ratio of useful energy gain per incident solar energy on the collector [28], which was defined as follows:

$$\eta_{coll} = \frac{Q_u}{A_C I} \quad (3)$$

where A_C is the collector's surface area (m^2) and I is the incident solar radiation intensity on the collector's absorber (Wm^{-2}). Q_u is the useful energy that the solar collector has collected, which was defined as follows:

$$Q_u = \dot{m} c_p \Delta T \quad (4)$$

where $\dot{m}$ is the passing air's mass flow rate in the collector (kgs^{-1}), c_p is the specific heat capacity ($J(kg^{\circ}C)^{-1}$) of drying air, and ΔT is the difference in drying air temperature between the inlet and outlet of the collector (°C).

2.4.3 The SEEC was determined by the ratio of electrical energy consumption per quantity of evaporated water from materials [11], which is defined as follows:

$$SEEC = \frac{EEC}{m_i - m_f} \quad (5)$$

where EEC is the electrical energy consumption (kWh) of the infrared source.

3. Results and Discussion

The Phlai drying experiments with a solar dryer combined with infrared radiation were conducted under various drying conditions. Temperature data at different points within the dryer and solar radiation intensity were collected during the drying period from December 2019 to April 2020. This article uses, as an example, only the drying condition: 70 °C PIT with 1500 W IRP, as shown in (Figure 5). Results from other drying conditions showed similar behavior. Environmental conditions during the experiment were as follows: ambient temperature ranged from 32 to 39 °C and averaged 37 °C, peaking at 2:00 PM, while radiation intensity varied from 590 to 1,200 Wm^{-2} and averaged 812 Wm^{-2}, with the highest level recorded at 11:30 AM.

Examination of air temperature measurements at various points indicated that the solar collector's inlet temperature (T_{ci}) was higher than the ambient temperature. This occurred because the drying system recovered waste thermal energy from the drying process, thus elevating the solar collector's inlet temperature (T_{ci}). The drying chamber's inlet temperature (T_{di}) was higher than the chamber's outlet temperature (T_{do}). Because the phlai slices were exposed to the drying air's heat and infrared radiation, the water evaporated, resulting in a slight decrease in the drying air temperature. The thermal energy storage unit's inlet temperature (T_{tsi}) was mostly higher than its outlet temperature (the drying chamber's inlet temperature, T_{di}). However, if the drying system does not have enough thermal energy or if the amount of solar radiation decreases, the stored thermal energy will be released as auxiliary energy, which will help stabilize the drying air temperature. It results in the drying chamber's inlet temperature being almost constant [2], which makes an infrared heater have less electrical energy consumption. These results were similar to those found by D.K. Rabha and P. Muthukumar [2], who studied the performance of a forced convection solar dryer combined with a paraffin wax-based shell and tube latent heat storage unit, which was tested from 8:00 to 18:00 o'clock. They discovered that on most bright sunny days, the charging process occurred between 8:00 and 14:30 o'clock.

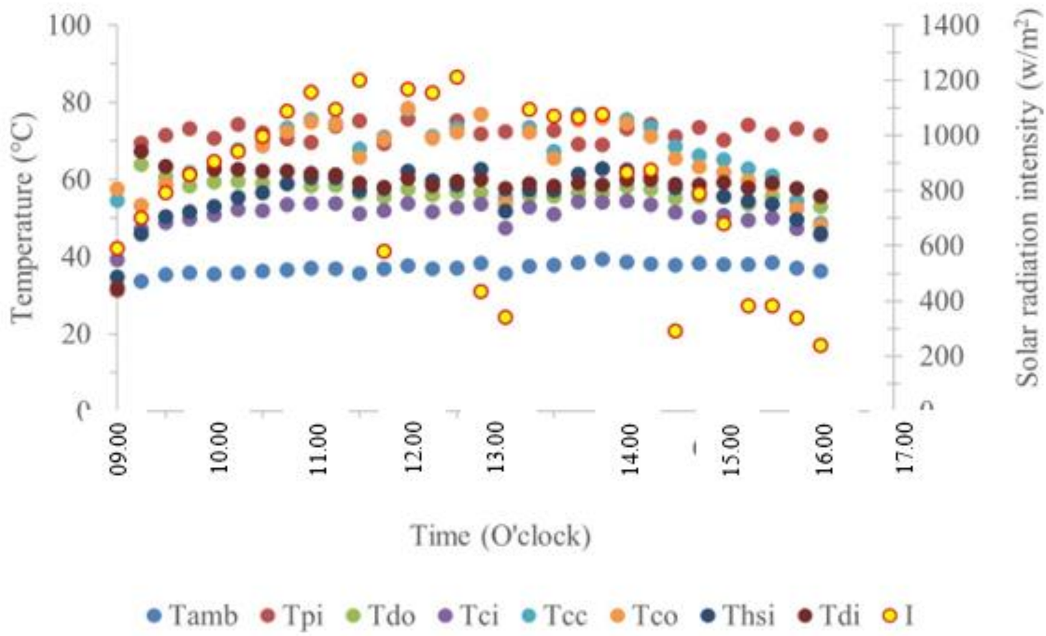

Figure 5 Drying air temperature at various points within the dryer, as well as solar radiation intensities, were collected during the experimental drying conditions at 70°C PIT and 1500 W IRP.

3.1 The performance of developed dryer

This hybrid solar dryer created hot air for water removal from materials by using solar thermal energy and was used in combination with the infrared drying technique, which is a high-efficiency and energy-saving method. In addition, a heat storage system and a waste heat recovery system were installed on this hybrid solar dryer, which can troubleshoot the instability problem of solar radiation and increase energy efficiency. The moisture content changes versus drying time under various drying conditions, as shown in (Figure 6).

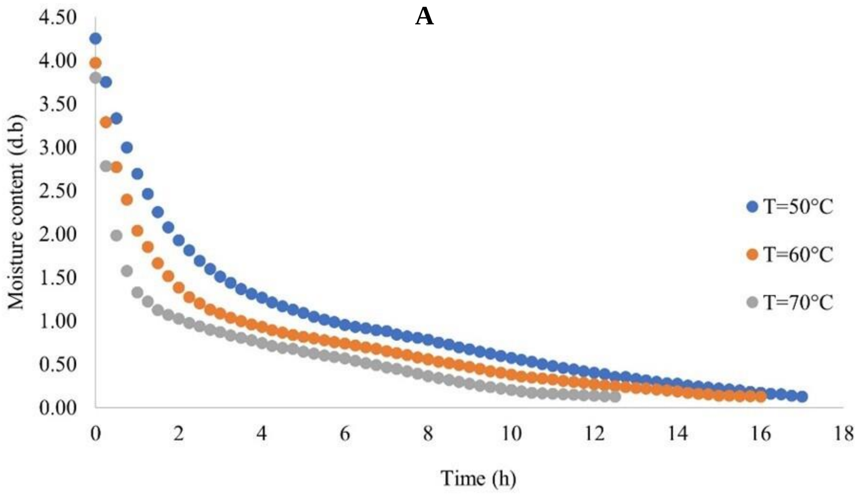

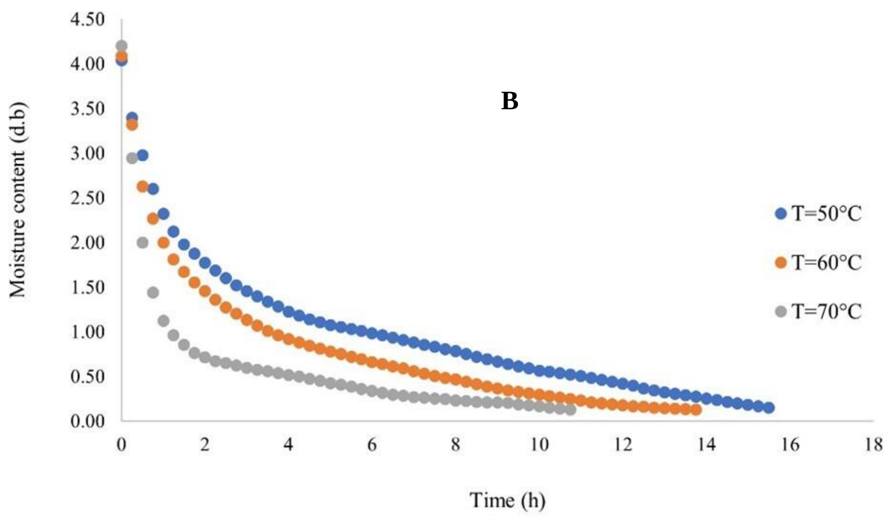

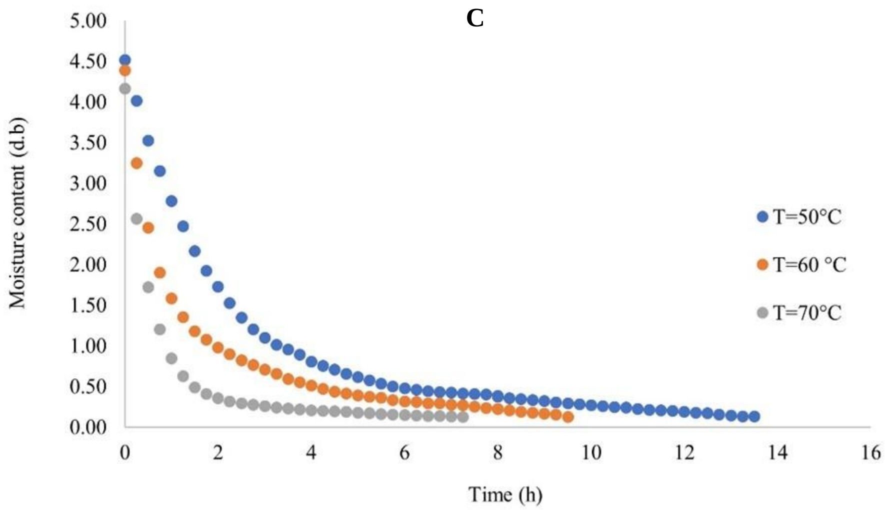

Figure 6 The moisture content changes versus drying time were observed at PITs of 50, 60, and 70 °C and

under IRPs of A) 500, B) 1000, and C) 1500 W.

The performance study of the developed dryer was determined from the t_d, the EEC, the DR, the η_{coll}, and the SEEC values, as shown in Table 1.

Table 1 The drying performance of the developed dryer.

IRP (W)	PIT (°C)	t_d (h)	EEC (kWh)	DR ($kg_{water}h^{-1}$)	η_{coll} (-)	SEEC ($kWhkg_{water}^{-1}$)
500	50	16.92±0.14[a]	0.51±0.07[de]	0.0047	64.36	7.28
	60	15.67±1.61[b]	0.89±0.14[b]	0.0051	70.43	13.57
	70	12.33±0.76[e]	1.38±0.19[a]	0.0067	53.36	14.15
1000	50	15.75±0.25[b]	0.36±0.18[ef]	0.0049	80.18	7.36
	60	13.30±0.80[d]	0.67±1.06[cd]	0.0061	83.69	8.54
	70	10.50±0.43[f]	0.97±0.04[b]	0.0077	56.98	12.16
1500	50	13.67±0.14[c]	0.19±0.06[f]	0.0070	69.65	1.58
	60	9.25±0.43[g]	0.55±0.03[de]	0.0082	76.69	8.32
	70	7.33±0.38[h]	0.78±0.09[bc]	0.0123	70.54	9.82

Mean ± SD (n = 3). Means labeled with different letters within each column indicate significant differences as determined by Duncan's New Multiple Range Test (DMRT) ($p<0.05$).

From Table 1, it was found that the t_d and EEC were in the range of 7.25 to 17.00 h and 0.150 to 1.156 kWh, respectively. In a study on the t_d of each drying condition, it was found that the drying condition at PIT of 70 °C with an IRP of 1500 W required the shortest time t_d of 7.25 h, while the drying condition at PIT of 50 °C with an IRP of 500 W took the longest time t_d of 17.00 h. The findings suggest that the t_d is inversely proportional to IRP and PIT. These results were similar to those of Lakchai et al. [29], who studied the effects of temperature and thickness on the hot air drying of sliced Phlai. They found that the drying time ranged from 28 to 36 h, and that an increase in temperature resulted in longer drying times. In a study on the amounts of EEC used in uneven infrared radiation sources, it was revealed that the drying conditions at PIT of 50 °C with an IRP of 1500 W gave the lowest amount of EEC at 0.150 kWh. The drying conditions at PIT of 70 °C with an IRP of 500 W gave the highest amount of EEC at 1.156 kWh. The experimental results show that drying at high PIT makes infrared sources use more electricity. Since the infrared sources are controlled based on the PIT, if the preset PIT is high, this will cause the infrared sources to use more electrical power to enable the PIT to reach the preset value. On the other hand, if the experiment's IRP is high, the EEC value used in infrared sources is reduced. Although conducting an experiment with a high IRP level will inevitably result in increased electricity consumption by the infrared sources, it also leads to a shorter drying process.

In terms of drying performances, it was found that the DR and SEEC values were between 0.0047 and 0.0123 $kg_{water}h^{-1}$ and 1.58 and 14.15 $kWhkg_{water}^{-1}$, respectively. Among the drying conditions, the highest DR value of 0.0123 $kg_{water}h^{-1}$ was achieved at a PIT of 70°C with an IRP of 1500 W, while the lowest DR value of 0.0047 $kg_{water}h^{-1}$ observed at a PIT of 50°C with an IRP of 500 W. This suggests that the DR value is directly proportional to both PIT and IRP. In SEEC values, the lowest value of 1.58 $kWhkg_{water}^{-1}$ was found at a PIT of 50°C with an IRP of 1500 W, while the highest SEEC value of 14.15 $kWhkg_{water}^{-1}$ was observed at a PIT of 70°C with an IRP of 500 W. The results show that the SEEC value was inversely proportional to the IRP and directly proportional to the PIT. The η_{coll} value was found to be between 53.36 and 83.69%. The experimental results showed that η_{coll} depends on drying conditions (PIT and IRP) and ambient conditions. These results were similar to those of Ziaforoughi and Esfahani [8], who studied drying potatoes using a solar dryer combined with intermittent infrared radiation. They found that the SEEC values ranged from 1.79 to 4.35 $kWhkg^{-1}$; an increase in temperature resulted in higher SEEC values.

4. Conclusion

This work investigated the development and efficiency of solar dryers combined with infrared radiation for Phlai drying. The results showed that the best drying conditions were at an IRP of 1500 W, which had the highest DR and the lowest SEEC. Two considerations arose from consideration of the PIT. - (1) from the perspective of electricity saving, the drying at PIT at 50 °C was optimal, yielding the lowest SEEC; and (2) from the perspective of drying time, the drying at PIT at 70 °C was optimal, yielding the highest DR.

Acknowledgement

The authors would like to thank the Department of Physics, Faculty of Science, Mahasarakham University, and the Program of Physics, Faculty of Science and Technology, Rajabhat Mahasarakham University, for supporting this research.

References

1. Rathi JO, Shankarling GS. Concentrated solar radiation aided energy efficient and chemoselective protocol for N-acylation and N-formylation reactions in aqueous medium. Sol. Energy. 2019;189:471-479.

2. Rabha DK, Muthukumar P. Performance studies on a forced convection solar dryer integrated with a paraffin wax–based latent heat storage system. Sol. Energy. 2017;149:214-226.
3. Nabnean S, Janjai S, Thepa S, Sudaprasert K, Songprakorp R, Bala BK. Experimental performance of a new design of solar dryer for drying osmotically dehydrated cherry tomatoes. Renew. Energy. 2016;94:147-156.
4. Umayal Sundari AR, Veeramanipriya E. Performance evaluation, morphological properties and drying kinetics of untreated Carica Papaya using solar hybrid dryer integrated with heat storage material. J. Energy Storage. 2022;55:1-18.
5. Ziaforoughi A, Esfahani JA. A salient reduction of energy consumption and drying time in a novel PV-solar collector-assisted intermittent infrared dryer. Sol. Energy. 2016;136:428-436.
6. Kowalski SJ, Mierzwa D. 2011. Drying of Osmotically Dehydrated Biological Materials. J. Agric. Mach. Sci. 2011;7(3):325-331.
7. Wang J, Sheng K. Far-infrared and microwave drying of peach. LWT-Food Sci. Technol. 2006;39(3):247-255.
8. Abdelbasset WK, Alrawaili SM, Elkholi SM, Eid MM, Abd-Elghany AA, Mahmoud MZ. The role of infrared waves in increasing the quality of food products. Food Sci. Technol. 2022;42:1-5.
9. Kumar C, Karim MA, Joardder MUH. Intermittent drying of food products: A critical Review. J. Food Eng. 2014;121:48-57.
10. Cetina-Quinones AJ, Lopez Lopez J, Ricalde-Cab L, Mekaoui AE, San-Pedro L, Bassam A. Experimental evaluation of an indirect type solar dryer for agricultural use in rural communities: Relative humidity comparative study under winter season in tropical climate with sensible heat storage material. Sol. Energy. 2021;224:58-75.
11. Aktas M, Sevik S, Amini A, Khanlari A. Analysis of drying of melon in a solar-heat recovery assisted infrared dryer. Sol. Energy. 2016;137:500-515.
12. Chaiyawatthanananthn P, Dechayont B, Phuaklee P, Ruangnoo S, Chunthorng-Orn, J. Anti-inflammatory pain-relieving activities of medicinal herbs used for hot salt pot compression. J Thai Trad Alt Med. 2020;18(3):455-469.
13. Chongmelaxme B, Sruamsiri R, Dilokthornsakul P, Dhippayom T, Kongkaew C, Saokaew S, Chuthaputti A, Chaiyakunapruk N. Clinical effects of Zingiber cassumunar (Plai): A systematic review. Complement Ther Med. 2017;35:70-77.
14. Singharach A, Thongpraditchote S, Anantachoke N, Temsiririrkkul R. Anti-inflammatory activity of Zingiber montanum (J.Konig) Link ex Dietr. extracts prepared by deep frying in coconut oil. Pharm Sci Asia. 2020;47(1):51-57.
15. Bhuiyan MdN, Chowdhury IJU, Jaripa Begum J. Volatile constituents of essential oils isolated from leaf and rhizome of Zingiber cassumunar Roxb. Bangladesh J. Pharmacol. 2008;3:69-73.
16. Meunathasa B, Paisooksantivatana Y, Manochai B. Effect of drying temperatures on quality of cassumunar ginger (Plai) rhizome (Zingiber montanum (Koenig) Link ex. Dietr.). Thai Agric. Res J.
17. 2011;29(1):59-72.
18. Mahayothee B, Thamsala T, Khuwijitjaru P, Janjai S. Effect of drying temperature and drying method on
19. drying rate and bioactive compounds in cassumunar ginger (Zingiber montanum). J. Appl. Res. Med.
20. Aromat. Plants. 2020;18:1-10.
21. Patrick T, Marcel E, Alexis K. Modelling and Numerical simulation of greenhouse effect in a solar collector with a W-Shape cover. Int. J. Energy Eng. 2020;10(2):59-66.
22. Gulcimen F, Karakaya H, Durmus A. Drying of sweet basil with solar air collectors. Renew. Energy. 2016;93:77-86.
23. Bolaji BO, Abiala I. Theoretical and experimental analyses of heat transfer in a flat-plate solar

collector. Walailak J Sci Technol. 2012;9(3):239-248.
24. Paminto J, Fianti, Yulianti I. The effect of surface color on the absorption of solar radiation. Phys. Comm. 2021;5(1):27-32.
25. Garcia RP, Oliveira SDR, Scalon VL. Thermal efficiency experimental evaluation of solar flat plate collectors when introducing convective barriers, Sol. Energy. 2019;182:278-285.
26. Younis M, Abdelkarim D, El-Abdein AZ. Kinetics and mathematical modeling of infrared thin-layer drying of garlic slices. Saudi J. Biol. Sci. 2018;25(2):332-338.
27. Agarwal A, Sarviya RM. An experimental investigation of shell and tube latent heat storage for solar dryer using paraffin wax as heat storage material. Eng. Sci. Technol. an Int. J. 2016;19:619-631.
28. Jouhara H, Khordehgah N, Almahmoud S, Delpech B, Chauhan A, Tassou SA. Waste heat recovery technologies and applications. Therm. Sci. Eng. Prog. 2018;6:268-289.
29. Nuimeem M, Soponronnarit S, Bunnag B. Optimum strategies for Pineapple glace. Witthayasan Kasetsat. 1993;27:79-90.
30. Adak N, Heybeli N, Ertekin C. Infrared drying of strawberry. Food Chem. 2017;219:109-116.
31. Altobelli F, Condorı M, Duran G, Martinez C. Solar dryer efficiency considering the total drying potential. Application of this potential as a resource indicator in north-western Argentina. Sol. Energy. 2014;105:742-759.
32. Lakchai A, Phaphuangwittayakul W, Viboon Changrue V, Sakulchangsatjatai P. Effects of temperature and
33. thickness on hot air drying of sliced Phlai (Zingiber cassumunar Roxb.). Agricultural Sci. J. 2008;39(3): 335-338.